Impaired Transition State Complementarity in the Hydrolysis of *O*-Arylphosphorothioates by Protein-Tyrosine Phosphatases†

Yan-Ling Zhang,‡ Florian Hollfelder,§,||,⊥ Steven J. Gordon,‡ Li Chen,‡ Yen-Fang Keng,‡ Li Wu,‡ Daniel Herschlag,|| and Zhong-Yin Zhang*,‡

Department of Molecular Pharmacology, Albert Einstein College of Medicine, 1300 Morris Park Avenue, Bronx, New York 10461, University Chemical Laboratory, Cambridge University, Lensfield Road, Cambridge, United Kingdom, CB2 1EW, and Department of Biochemistry, Beckman Center B400, Stanford University, Stanford, California 94305

Received April 9, 1999; Revised Manuscript Received June 23, 1999

ABSTRACT: The hydrolysis of *O*-arylphosphorothioates by protein-tyrosine phosphatases (PTPases) was studied with the aim of providing a mechanistic framework for the reactions of this important class of substrate analogues. *O*-Arylphosphorothioates are hydrolyzed 2 to 3 orders of magnitude slower than *O*-aryl phosphates by PTPases. This is in contrast to the solution reaction where phosphorothioates display 10−60-fold higher reactivity than the corresponding oxygen analogues. Kinetic analyses suggest that PTPases utilize the same active site and similar kinetic and chemical mechanisms for the hydrolysis of *O*-arylphosphorothioates and *O*-aryl phosphates. Thio substitution has no effect on the affinity of substrate or product for the PTPases. Brønsted analyses suggest that like the PTPase-catalyzed phosphoryl transfer reaction the transition state for the PTPase-catalyzed thiophosphoryl transfer is highly dissociative, similar to that of the corresponding solution reaction. The side chain of the active-site Arg residue forms a bidentate hydrogen bond with two of the terminal phosphate oxygens in the ground state and two of the equatorial oxygens in a transition state analog complex with vanadate [Denu et al. (1996) *Proc. Natl. Acad. Sci. USA 93*, 2493−2498; Zhang, M. et al. (1997) *Biochemistry 36*, 15−23; Pannifer et al. (1998) *J. Biol. Chem. 273*, 10454−10462]. Replacement of the active-site Arg409 in the *Yersinia* PTPase by a Lys reduces the thio effect by 54-fold, consistent with direct interaction and demonstrating strong energetic coupling between Arg409 and the phosphoryl oxygens in the transition state. These results suggest that the large thio effect observed in the PTPase reaction is the result of inability to achieve precise transition state complementarity in the enzyme active site with the larger sulfur substitution.

Protein tyrosine phosphatases (PTPases)[1] catalyze the removal of the phosphoryl group from aryl phosphates and phosphotyrosine in peptides/proteins. The PTPase superfamily includes the classical tyrosine-specific PTPases, the dual specificity phosphatases, and the low molecular weight phosphatases. These three groups of phosphatases share the signature motif (H/V)**C**(X)$_5$**R**(S/T) and other key structural features that are important for catalysis and are believed to utilize a common mechanism to effect catalysis (*1*). In this mechanism (Figure 1), the side chain of the active-site Cys residue serves as a nucleophile to accept the phosphoryl group from the substrate and form a kinetically competent cysteinyl phosphate intermediate (*2*, *3*). The active-site Arg residue interacts with the phosphoryl moiety of the substrate and plays a role in both substrate binding and transition state stabilization (*4*). To facilitate substrate turnover, PTPases also employ an invariant Asp residue, which acts as a general acid by protonating the ester oxygen of the leaving group leading to the formation of the cysteinyl phosphate intermediate (*5*). The phosphoenzyme intermediate is subsequently hydrolyzed by a water molecule, which is activated by the same conserved Asp residue.

Substantial physical organic evidence suggests that the nonenzymatic solution reaction of the dianion of phosphate monoesters proceeds through a concerted mechanism with a mostly dissociative transition state (Scheme 1) in which

‡ Albert Einstein College of Medicine.
§ Cambridge University.
|| Stanford University.
⊥ Present address: Department of Molecular Pharmacology and Biological Chemistry, Harvard Medical School, 240 Longwood Avenue, MA 02115, USA.

† This work was supported by National Institutes of Health Grant CA69202 (to Z.-Y. Z.) and in part by a David and Lucile Packard Foundation Fellowship in Science and Engineering (to D. H.). Z.-Y. Z. is a Sinsheimer Scholar and an Irma T. Hirschl Career Scientist. F. H. is the Walter Grant Scott Research Fellow in Bioorganic Chemistry at Trinity Hall, Cambridge, United Kingdom and recipient of a Marie-Curie Fellowship of the European Commission.

* To whom correspondence should be addressed. Phone: 718-430-4288. FAX: 718-430-8922. E-mail: zyzhang@aecom.yu.edu.

[1] Abbreviations: PTPase, protein-tyrosine phosphatase; LAR, leukocyte common antigen-related; PTP1B, protein tyrosine phosphatase 1B; Stp1, small tyrosine phosphatase 1; VHR, VH1-related; *p*NPP, *p*-nitrophenyl phosphate; *p*NPP(S), *p*-nitrophenyl phosphorothioate, E−P, phosphocysteinyl enzyme intermediate; E−P(S), thiophosphocysteinyl enzyme intermediate; SDS-PAGE, sodium dodecyl sulfate-polyacrylamide gel electrophoresis; CHES, 3-(cyclohexylamino)-ethanesulfonic acid; HEPES, 4-(2-hydroxyethyl)-1-piperazineethanesulfonic acid; EDTA, ethylenediaminetetraacetic acid.

10.1021/bi990836i CCC: $18.00
Published on Web 08/26/1999

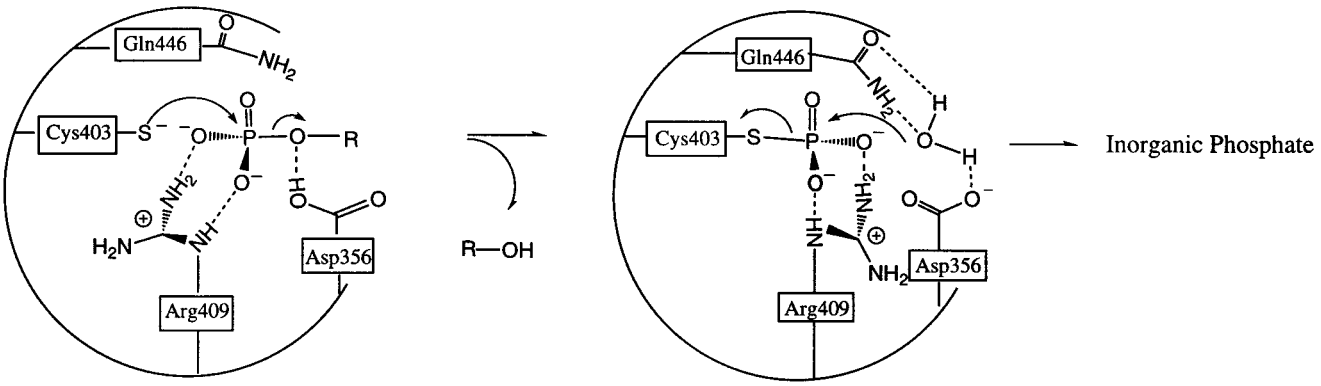

FIGURE 1: A chemical mechanism for the *Yersinia* PTPase-catalyzed hydrolysis of pNPP.

Scheme 1

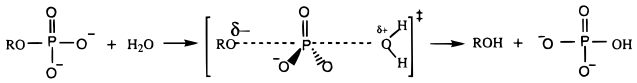

bond formation to the incoming nucleophile is minimal and bond breaking between the phosphorus and the leaving group is substantial (*6*−*9*). Recent heavy atom kinetic isotope effect measurements and Brønsted correlation studies on the PTPase-catalyzed reaction suggest that the nature of the enzymatic transition state is similar to that of the uncatalyzed solution reaction (*10*−*13*). Thus, the transition state of the solution reaction is essentially the one stabilized by the enzyme leading to catalysis.

O-Phosphorothioate monoesters, in which a nonbridge oxygen atom of the phosphate group is replaced by a sulfur atom, exhibit approximately 10−60-fold enhanced intrinsic chemical reactivity in solution (*14*−*16*). This inverse thio effect (the ratio of the rate of phosphate ester vs phosphorothioate ester reaction) can be rationalized by the higher electronegativity of oxygen as compared to sulfur.[2] Thio substitution speeds up dissociative reactions that require electron donation from the phosphoryl substituents and slows down associative reactions in which electron withdrawal from the phosphorus stabilizes the transition state (*17*). Nevertheless, *O*-phosphorothioate monoesters were found to be less reactive compared to phosphate esters in PTPase-catalyzed reactions (*18*−*23*). In other words, thio substitution increases solution hydrolysis but decreases the enzymatic reaction. The stability of phosphorothioates toward PTPases has been useful for the investigation of the role of tyrosine phosphorylation in cell signaling (*18*). Thiophosphorylated lysozyme coupled to a stationary phase has been used as an affinity column that led to the purification of the first PTPase (*19*). Yet to date, detailed study of the molecular basis for the large thio effect in the PTPase reaction was lacking.

This work was designed to fully characterize the PTPase-catalyzed phosphorothioate reaction and compare it with the well-characterized phosphate reaction. The results suggest that the hydrolysis of *O*-arylphosphorothioates by PTPases follows the same mechanistic pathway as that of phosphate monoesters, and the nature of the transition state for phosphorothioates hydrolysis catalyzed by these enzymes is dissociative, similar to that in solution. Analysis of the differential thio effects associated with the wild-type and a number of site-directed mutant *Yersinia* PTPases suggests that sulfur substitution disrupts the geometric complementarity between the active-site Arg residue and the phosphoryl oxygens in the transition state, providing a molecular explanation for the reduced reactivity of *O*-arylphosphorothioates in the PTPase reaction.

[2] It should be recognized that electronegativity alone does not explain all properties of phosphorothioates. For example, the sulfur atom in phosphorothioates carries a full negative charge and polarizability is probably a more important factor than electronegativity in determining the electronic nature of these compounds (see ref *67*).

EXPERIMENTAL PROCEDURES

Enzymes and Chemicals. The wild-type *Yersinia* PTPase, PTP1B, VHR, Stp1, LAR and *Yersinia* PTPase mutants Q446A, Q450A, D356A, W354A, and R409K were expressed under the control of the T7 promoter in *Escherichia coli* BL21(DE3) and grown at room temperature after induction with 0.4 mM IPTG. All recombinant proteins were purified to greater than 95% purity as described previously (*24*−*28*). *p*-Nitrophenyl phosphate (*p*NPP) was purchased from Fluka. Sodium thiophosphate, deuterium oxide, ethylene glycol, 2,2,2-trifluoroethanol, propargyl alcohol, allyl alcohol, and 2-propanol were purchased from Aldrich. Phenyl phosphate, cyanoethanol, 2-methoxyethanol, and ethyl alcohol were purchased from Sigma. Substituted pyridines were from Aldrich in highest purity available and distilled prior to use.

Synthesis. Cyclohexylammonium salts of 4-nitrophenyl, 2,4-dichlorophenyl, 4-cyanophenyl, 3-nitrophenyl, 2-chlorophenyl, 4-chlorophenyl, 4-fluorophenyl, phenyl, and 3,4-dimethylphenyl phosphorothioates were prepared as previously described (*16*), except for the following modification. The crude phosphorodichloridite was dissolved in 20 mL dioxane and cooled to 0 °C before sodium hydroxide was added. This helped to homogenize the hydrolysis mixture, facilitated removal of water as an azeotropic mixture and led to product of higher purity. Aryl phosphate monoesters: 4-nitrophenyl, 2,4-dichlorophenyl, 4-cyanophenyl, 3-nitrophenyl, 2-chlorophenyl, 4-chlorophenyl, 3,4-dimethylphenyl, and 4-fluorophenyl phosphate were synthesized as described (*29*).

Detection of Reaction Products by ^{31}P NMR. Hydrolyses of thiophosphate and *p*-nitrophenyl phosphorothioate [*p*NPP(S)] were monitored on a Bruker DRX 300 MHz spectrometer at 27 °C using the following parameters: acquisition time 0.28 s, delay time 0.8 s, spectral width 14,620 Hz (120 ppm). All spectra were recorded with H-decoupling. The chemical shift of inorganic phosphate in D_2O was set to zero. The concentration of *p*NPP(S) was 5

mM and the concentration of thiophosphate was 5 or 32 mM. The enzyme and substrate were dissolved in a 50 mM succinate, 1 mM EDTA, pH 6.0 buffer, containing 20% D_2O. The rate of enzymatic hydrolysis of thiophosphate was determined by measuring the appearance of inorganic phosphate. This was based on the observation that substitution of oxygen for sulfur in inorganic phosphate causes a dramatic downfield chemical shift from 2 to 40 ppm. The hydrolysis reaction was initiated by addition of *Yersinia* PTPase (4.2 μM), PTP1B (3.5 μM), or VHR (7.0 μM) to a reaction mixture containing 32 mM thiophosphate. To demonstrate the transfer of thiophosphate from *p*NPP(S) to an exemplary alcohol, 1 M ethylene glycol was included in the NMR sample (*25*).

Steady-State Kinetics. Initial rates for the hydrolysis of *p*NPP and other aryl phosphate monoesters by the *Yersinia* PTPase, PTP1B, VHR, Stp1, and LAR were measured as described previously (*24*, *30*). Initial rates for the enzymatic hydrolysis of *p*NPP(S) and other aryl phosphothioate monoesters were measured by following the absorbance from 279 to 410 nm at the wavelength giving the largest change in absorbance. The nonenzymatic hydrolysis of the substrates was corrected by measuring the control without the addition of the enzyme. The extinction coefficients were determined by following the absorbance at the corresponding wavelength for complete hydrolysis of aryl phosphothioates or their phosphate substrates. The extinction coefficients for the corresponding phenolate products of these arylphosphothioate monoesters were determined in 1 N NaOH as follows (in unit of M^{-1} cm^{-1}): $\epsilon_{405} = 18\,000$ for 4-nitrophenolate, $\epsilon_{306} = 4300$ for 2,4-dichlorophenolate, $\epsilon_{280} = 20\,000$ for 4-cyanophenolate, $\epsilon_{400} = 1430$ for 3-nitrophenolate, $\epsilon_{293} = 2800$ for 2-chlorophenolate, $\epsilon_{300} = 3460$ for 4-chlorophenolate, $\epsilon_{300} = 3120$ for 4-fluorophenolate, $\epsilon_{285} = 1220$ for 3,4-dimethylphenolate, and $\epsilon_{285} = 2340$ for phenolate.

Buffers used were as follows: pH 4.0 and 5.0, 100 mM acetate; pH 6.0, 50 mM succinate; pH 7.0, 50 mM 3,3-dimethyglutarate; pH 8.0 and 9.0, 100 mM Tris. All of the buffer systems contained 1 mM EDTA, and the ionic strength of the solutions were kept at 0.15 M using NaCl. The enzyme concentration was determined from the absorbance at 280 nm using $A_{1mg/mL}^{280}$ (absorbance at 280 nm for a 1 mg/mL solution) of 0.493, 1.24, 0.564, 0.724, and 1.28 for *Yersinia* PTPases, PTP1B, VHR, Stp1, and LAR, respectively. The W354A mutant *Yersinia* PTPase has an $A_{1mg/mL}^{280}$ of 0.24 because of the substitution of the tryptophan residue. The Michaelis−Menten kinetic parameters were determined from a direct fit of the velocity vs [S] data to the Michaelis−Menten equation using the nonlinear regression program KinetAsyst (IntelliKinetics, State College, PA). The range of *O*-arylphosphorothioate concentration used was from 0.4 to 10 mM. The range of *O*-aryl phosphate concentration used was from 0.2 to 5 K_m. In all cases, the enzyme concentration was much lower than that of the substrate so that the steady-state assumption was fulfilled. Inhibition constants (K_i) for the PTPase by inorganic phosphate, thiophosphate, and *p*NPP(S) were determined with *p*NPP as substrate at pH 6.0 and 30 °C. The mode of inhibition and K_i value were determined in the following manner. At various fixed concentrations of inhibitor (0 to 3 K_i), the initial rate at a series of *p*NPP concentrations was measured ranging from 0.2 to 5 the apparent K_m values. The data were fitted to appropriate equations using KinetAsyst to obtain the inhibition constant and to assess the mode of inhibition.

Scheme 2

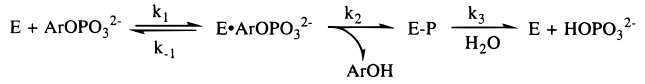

Determination of Second-Order Rate Constants for the Pyridine-Catalyzed Reaction of pNPP(*S*) *and the First-Order Rate Constant for the Nonenzymatic Hydrolysis of pNPP*(*S*). The amine-catalyzed hydrolysis of *p*NPP(S) cyclohexylammonium dianion (55 μM) was studied with a series of pyridines at 37 °C at constant ionic strength ([KCl] = 1 M) in CHES buffer (50 mM, pH 9.41). First-order rate constants were measured and plotted against the relevant pyridine concentration to obtain the second-order rate constant as the slope. Second-order plots were linear over the concentration ranges employed (0 up to 0.0475−0.475 M, depending on pyridine solubility). This second-order rate constant was then used in the Brønsted correlation (Figure 5 below). No correction was made for pyridine self-association (*33*). Such a correction would correspond to a 0.3 unit change in log *k* for the strongly associating methylpyridines at the concentration empolyed but was not made as the data were better fit by a linear dependence on pyridine concentration.

Pre-Steady-State Kinetics. Pre-steady-state kinetic measurements of the wild-type *Yersinia* PTPase and its Q446A mutant, PTP1B, and VHR-catalyzed hydrolysis of *p*NPP(S) and *p*NPP were conducted at pH 6.0 and 30 °C. The reaction was monitored by the increase in absorbance at 405 nm of the *p*-nitrophenolate product. The enzyme concentration after mixing was 54, 72, and 89 μM for the *Yersinia* PTPase, PTP1B, and VHR, respectively. The concentrations for *p*NPP(S) and *p*NPP after mixing were 5 and 26 mM, respectively. The extinction coefficient for the mixture of *p*-nitrophenolate/*p*-nitrophenol at 405 nm is 1,300 M^{-1} cm^{-1} at pH 6.0 and 30 °C. When PTPase and *p*NPP or *p*NPP(S) are rapidly mixed in a stopped-flow spectrophotometer, the increase in absorbance at 405 nm as a function of time can be described as: $\text{Absorbance}_{405nm} = A \times t + B \times (1 - e^{-b \times t}) + C$. The burst amplitudes and rate constants were evaluated by the procedure described in (*31*). The correlation between the kinetic parameters [burst amplitude (B), transient rate constant (b) and the rate constant of the slow phase (A)], and the kinetic mechanism defined by Scheme 2 are described by equations (1) to (4):

$$A = \epsilon \times [E_0] \times k_{cat} \times \frac{[S_0]}{[S_0] + K_m} \quad (1)$$

$$B = \epsilon \times [E_0] \times \left[\frac{k_2/(k_2 + k_3)}{1 + K_m/[S_0]}\right]^2 \quad (2)$$

$$b = k_3 + \frac{k_2}{(1 + K_m/[S_0])} \quad (3)$$

$$k_{cat} = \frac{k_2 \times k_3}{k_2 + k_3} \quad (4)$$

E is the enzyme, $ArOPO_3^{2-}$ the substrate, $E{\cdot}ArOPO_3^{2-}$ the enzyme-substrate Michaelis complex, E−P, the phospho-

Table 1: Comparison of Steady-State Kinetic Parameters of Enzymatic Hydrolysis of *p*NPP and *p*NPP(S)

enzyme	substrate	k_{cat} (s^{-1})	K_m (mM)	k_{cat}/K_m (M^{-1} s^{-1})	thioeffect[a]
Yersinia PTP	*p*NPP	345 ± 5	2.6 ± 0.1	1.3×10^5	5.0×10^3
	*p*NPP(S)	$(7.0 \pm 0.8) \times 10^{-2}$	2.7 ± 0.6	26	
PTP1B	*p*NPP	34 ± 1	0.91 ± 0.01	3.7×10^4	2.3×10^3
	*p*NPP(S)	$(4.3 \pm 0.1) \times 10^{-2}$	2.7 ± 0.2	16	
LAR	*p*NPP	12 ± 1	1.9 ± 0.1	6.3×10^3	1.0×10^3
	*p*NPP(S)	$(1.8 \pm 0.1) \times 10^{-2}$	3.0 ± 0.3	6.0	
VHR	*p*NPP	6.0 ± 0.5	1.7 ± 0.1	3.5×10^3	67
	*p*NPP(S)	$(3.1 \pm 0.1) \times 10^{-2}$	0.6 ± 0.1	52	
Stp1	*p*NPP	2.4 ± 0.2	0.08 ± 0.01	3.0×10^4	2.1×10^2
	*p*NPP(S)	$(3.3 \pm 0.1) \times 10^{-2}$	0.23 ± 0.02	1.4×10^2	

[a] The thio effect is defined as $(k_{cat}/K_m)_{pNPP}/(k_{cat}/K_m)_{pNPP(S)}$. All measurements were at pH 6.0 and 30 °C. Errors for individual kinetic experiments were obtained from the direct nonlinear regression fit of the data to the Michelis−Menten equation. The reported values were the average of three independent experiments and the errors are standard deviations.

enzyme intermediate, and ArOH, the phenol. When substrate concentration is sufficiently higher than K_m, eqs 1, 2, and 3 reduce to eqs 5−7; ϵ is the extinction coefficient of the monitored product at the indicated wavelength, and $[E_0]$ and $[S_0]$ are the initial enzyme and substrate concentrations. Enzyme, substrate, and enzyme−substrate complex are assumed in a fast preequilibrium. Thus, the values of all reaction parameters can be determined using these equations.

$$A = \epsilon \times [E_0] \times k_{cat} \quad (5)$$

$$B = \epsilon \times [E_0] \times \left[\frac{k_2}{k_2 + k_3}\right]^2 \quad (6)$$

$$b = k_3 + k_2 \quad (7)$$

Determination of Second-Order Rate Constants for the Thiophosphoryl Transfer Reaction from the Thiophosphoenzyme Intermediate to Various Alcohols. The rate-limiting step for *Yersinia* PTPase Q446A-catalyzed hydrolysis of *p*NPP(S) is the breakdown of the phosphoenzyme intermediate, similar to the hydrolysis of *p*NPP by the PTPase (*25*). Under this condition, the observed k_{cat} value for the *p*NPP(S) reaction in the presence of alcohols as determined by following the production of *p*-nitrophenolate is the sum of the individual rate constants for the thiophosphoenzyme hydrolysis and thiophosphoryl transfer to alcohol (*25*). The alcohol concentrations employed were from 0 to 0.8 M. Typically, the rate increase in the presence of alcohol ranged from 20 to 80% of the hydrolysis reaction. A plot of k_{cat} against alcohol concentration is linear with an intercept at the rate of hydrolysis. The slope of this line is the second-order rate constant for the reaction of thiophosphoenzyme with alcohol (*13*).

D_2O Solvent Isotope Effect. The steady-state solvent kinetic isotope experiments were conducted in the equivalent buffer of pH 6.0, 50 mM succinate, 1 mM EDTA, $I = 0.15$ M. Buffer solutions in heavy water (100 mL) were prepared as follows: 100 mL of the pH 6.0 buffer was lyophilized to dryness, redissolved in 20 mL of D_2O and lyophilized to dryness two times and then dissolved in 100 mL of D_2O. As predicted by theory, the pH meter reading of the buffered D_2O solution was 6.1 and the corresponding pD value = pH meter reading + 0.4 = 6.5 (*32*).

RESULTS

Thio Effect for the PTPase-Catalyzed Hydrolysis of p-Nitrophenylphosphorothioate. We establish in the following the steady-state parameters, catalytic sequence, and nature of the transition state for the phosphorothioate vs phosphate ester hydrolysis by the PTPases. This forms the basis for a molecular analysis of the thio effect, which is further probed by a comparison between the wild-type and mutant enzymes. To assess the magnitude of the thio effect, steady-state parameters for the PTPase-catalyzed hydrolysis of *p*-nitrophenyl phosphate (*p*NPP) and *p*-nitrophenylphosphorothioate [*p*NPP(S)] were compared. At pH 6.0 and 30 °C, the k_{cat} values for the *Yersinia* PTPase-catalyzed hydrolysis of *p*NPP and *p*NPP(S) were 345 and 0.07 s^{-1}, respectively. The K_m for *p*NPP(S) was 2.7 mM, similar to that for *p*NPP (Table 1). Thus, replacing a nonbridge oxygen in *p*NPP by a sulfur atom decreases both k_{cat} and k_{cat}/K_m by 5000-fold in the *Yersinia* PTPase-catalyzed reaction. For comparison, the first-order rate constant for the solution hydrolysis of the dianion of *p*NPP(S) at 37 °C was determined to be 2.2×10^{-7} s^{-1}. The rate constant for the solution reaction of the dianion of *p*NPP was 1.6×10^{-8} s^{-1} at 39 °C (*33*). Thus, the *Yersinia* PTPase enhances the rates of *p*NPP hydrolysis by $\sim 10^{10}$ and catalyzes the hydrolysis of *p*NPP(S) over the solution reaction by $\sim 10^5$.

To determine if the reduced activity toward phosphorothioates is a unique property of the *Yersinia* PTPase, we also measured the kinetic parameters for the hydrolysis of *p*NPP(S) by several other PTPases. As summarized in Table 1, the mammalian tyrosine-specific phosphatases PTP1B and LAR, the human dual specificity phosphatase VHR, and the yeast low molecular weight phosphatase Stp1 all exhibited reduced k_{cat} values in the range between 0.02 and 0.04 s^{-1} for *p*NPP(S), which were similar to that of the *Yersinia* PTPase. In addition, the K_m values for *p*NPP(S) were not significantly different from those of *p*NPP.

PTPases Use the Same Active Site in Hydrolyzing pNPP(S) and pNPP. To exclude the possibility that the low activity toward phosphorothioates is due to contaminating phosphatases in the recombinant PTPase preparations, we tested a catalytically inactive mutant PTPase. Mutations at the active-site Cys residue destroy the PTPase's ability to hydrolyze *p*NPP and pTyr-containing protein substrates (*34*). A purified preparation of the catalytically inactive C403S mutant of *Yersinia* PTPase was also unable to hydrolyze *p*NPP(S). Furthermore, various catalytically impaired *Yersinia* PTPases exhibited activity toward *p*NPP(S) different from that of the wild-type enzyme (see below). Finally, inorganic phosphate binds to the active site and behaves as a competitive inhibitor of PTPases. The inhibition constants

Table 2: Inhibition of the PTPases by Thiophosphate and *p*NPP(S)[a]

enzyme	inhibitor	K_i (mM)	K_m (mM)
Yersinia PTPase	inorganic phosphate	15 ± 1	
	thiophosphate	6.4 ± 0.3	
	*p*NPP(S)	1.2 ± 0.1	2.7 ± 0.6
PTP1B	inorganic phosphate	28 ± 3	
	thiophosphate	7.1 ± 0.2	
	*p*NPP(S)	1.6 ± 0.3	2.7 ± 0.2
VHR	inorganic phosphate	1.0 ± 0.1	
	thiophosphate	3.2 ± 0.4	
	*p*NPP(S)	2.0 ± 0.2	0.6 ± 0.1

[a] All measurements were at pH 6.0 and 30 °C. Errors for each K_i measurement were obtained from the direct nonlinear regression fit of the data to appropriate equations using KinetAsyst. The reported values were the average of three independent experiments and the errors were standard deviations. For experimental details, see Experimental Procedures.

of inorganic phosphate for the *p*NPP and *p*NPP(S) reactions were identical, consistent with a common active site. Collectively, these results suggest that PTPases use the same active site to hydrolyze phosphate and phosphorothioates.

Affinity of Phosphorothioates for PTPases. We compared the binding of phosphate and thiophosphate by using these compounds as inhibitors of the *p*NPP reaction. Kinetic analysis showed that both phosphate and thiophosphate were competitive inhibitors. The K_i values are similar for phosphate and thiophosphate (Table 2). In addition, the K_m values for *p*NPP and *p*NPP(S) are also similar. Thus, the results suggest that the thio substitutions have no significant effect on ground-state binding.

Characterization of Reaction Pathway and Catalytic Sequence. Since the PTPase-catalyzed phosphate monoester hydrolysis proceeds through two distinct chemical steps via a cysteinyl phosphate intermediate (Figure 1 and Scheme 2), we first established whether phosphorothioates were hydrolyzed by a similar sequence. One of the products from the hydrolysis of *O*-arylphosphorothioates is thiophosphate. Since PTPases can catalyze the ^{18}O exchange reaction between inorganic phosphate and water (*29*, *35*, *36*), we determined whether thiophosphate could be hydrolyzed by PTPases. Indeed, thiophosphate was not stable in the presence of the enzyme and was hydrolyzed to inorganic phosphate and H_2S by the *Yersinia* PTPase as shown by ^{31}P NMR experiments (Figure 2A). The k_{cat} values for the hydrolysis of thiophosphate by the *Yersinia* PTPase, PTP1B, and VHR were 0.32, 0.063, and 0.16 s^{-1}, respectively, at pH 6.0 and 27 °C (Table 3). The solution hydrolysis of thiophosphate was insignificant under the same condition (data not shown); the rate of thiophosphate hydrolysis in solution at pH 6.0 and 53 °C was previously determined to be 4.3×10^{-5} s^{-1} (*37*).

Figure 2B shows the ^{31}P NMR spectra of the *Yersinia* PTPase-catalyzed hydrolysis of *p*NPP(S). Three phosphorus-containing species represented by three individual NMR peaks were present during the hydrolysis of *p*NPP(S). On the basis of the chemical shifts of inorganic phosphate (~2 ppm) and thiophosphate (40 ppm), the peak at 42 ppm was assigned to *p*NPP(S). In the presence of the *Yersinia* PTPase, *p*NPP(S) decreased with time as inorganic phosphate increased with time. In addition, there was a rapid increase in thiophosphate concentration, which then stayed at a constant steady-state level (Figure 2B and C). A comparison of the

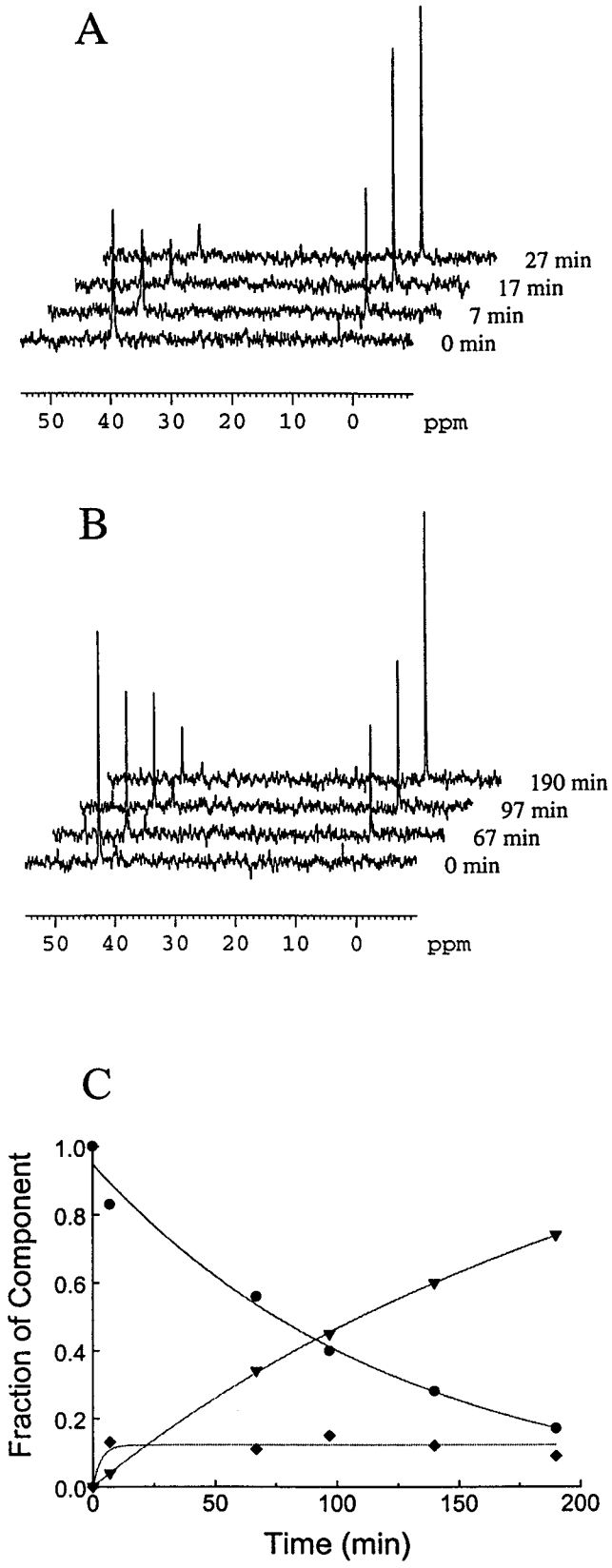

FIGURE 2: Time course of the *Yersinia* PTPase-catalyzed hydrolysis of thiophosphate (A) and *p*NPP(S) (B) at pH 6.0, 27 °C. The concentration of thiophosphate and pNPP(S) was 5 mM, while the concentration for *Yersinia* PTPase was 29 μM. ^{31}P NMR chemical shifts of thiophosphate, *p*NPP(S), and inorganic phosphate were 40, 42, and 2 ppm, respectively. (C), the mole fractions (determined from integration of corresponding NMR signals) of reactant (*p*NPP(S), ●), intermediate (thiophosphate, ◆), and product (inorganic phosphate, ▲).

Table 3: Comparison of the Rates of the PTPase-catalyzed Hydrolysis of Inorganic Phosphate and Thiophosphate

enzyme	substrate	k_{cat} (s^{-1})
Yersinia PTPase	inorganic phosphate	0.77 ± 0.05[a]
	thiophosphate	0.32 ± 0.03[b]
PTP1B	inorganic phosphate	0.014 ± 0.002[c]
	thiophosphate	0.063 ± 0.006[b]
VHR	thiophosphate	0.16 ± 0.02[b]

[a] Measured at pH 6.0 and 23 °C (*35*). [b] Measured at pH 6.0 and 27 °C. [c] Measured at pH 6.0 and 23 °C (*36*).

time course for the disappearance of thiophosphate (Figure 2A) and *p*NPP(S) (Figure 2B) indicated that the *Yersinia* PTPase-catalyzed hydrolysis of *p*NPP(S) was slower than that of thiophosphate. These results suggest that thiophosphate is an intermediate in the reaction that is first produced from *p*NPP(S) and subsequently hydrolyzed to yield inorganic phosphate upon the action of the PTPase. Similar results were obtained for the hydrolysis of *p*NPP(S) by VHR and PTP1B.

Although *p*NPP(S) is more than 3 orders of magnitudes less reactive than *p*NPP toward the *Yersinia* PTPase and PTP1B, the k_{cat} values for PTPase-catalyzed hydrolysis of thiophosphate were similar to the k_{cat} values for the enzyme-catalyzed ^{18}O exchange between inorganic phosphate and water (Table 3). A similar observation was made with the alkaline phosphatase-catalyzed thiophosphate hydrolysis (*38*). This may be rationalized by the notion that sulfur in the thiophosphate reaction has become the leaving group rather than a substituent of one of the nonbridge phosphoryl oxygens. The weaker P−SH bond than P−OH bond may be compensated for by the thio effect diminishing protonation of the sulfur leaving group (e.g., $pK_a^{SH^-} = 6.9$ and $pK_a^{OH^-} = 15.7$).

Rate-Limiting Step of the PTPase-Catalyzed pNPP(S) Hydrolysis. Burst kinetics have been observed at 3−4 °C for the hydrolysis of *p*NPP catalyzed by the *Yersinia* PTPase and PTP1B (*30*, *36*). It is suggested that under these conditions, the hydrolysis of the phosphocysteinyl enzyme intermediate (E−P in Scheme 2) is rate-limiting. This reaction was too fast for the detection of the transient burst phase of phenol liberation at room temperature. Because *p*NPP(S) is 3 orders of magnitude less reactive than *p*NPP in the PTPase reaction and has similar affinity as *p*NPP for the phosphatases, we suspected that it might be possible to study the pre-steady-state kinetics of the PTPase-catalyzed *p*NPP(S) hydrolysis reaction at higher temperatures. Indeed, we observed significant transient phase using *p*NPP(S) as a substrate in the *Yersinia* PTPase reaction at 30 °C and pH 6.0 (Figure 3A). The appearance of a burst pattern of phenol formation is consistent with the breakdown of the thiophosphocysteinyl enzyme intermediate [E−P(S)] (Scheme 3, k_3') being rate-limiting.[3] Kinetic analysis yielded a rate constant 3.4 s^{-1} for the burst phase, which was 50-fold faster than

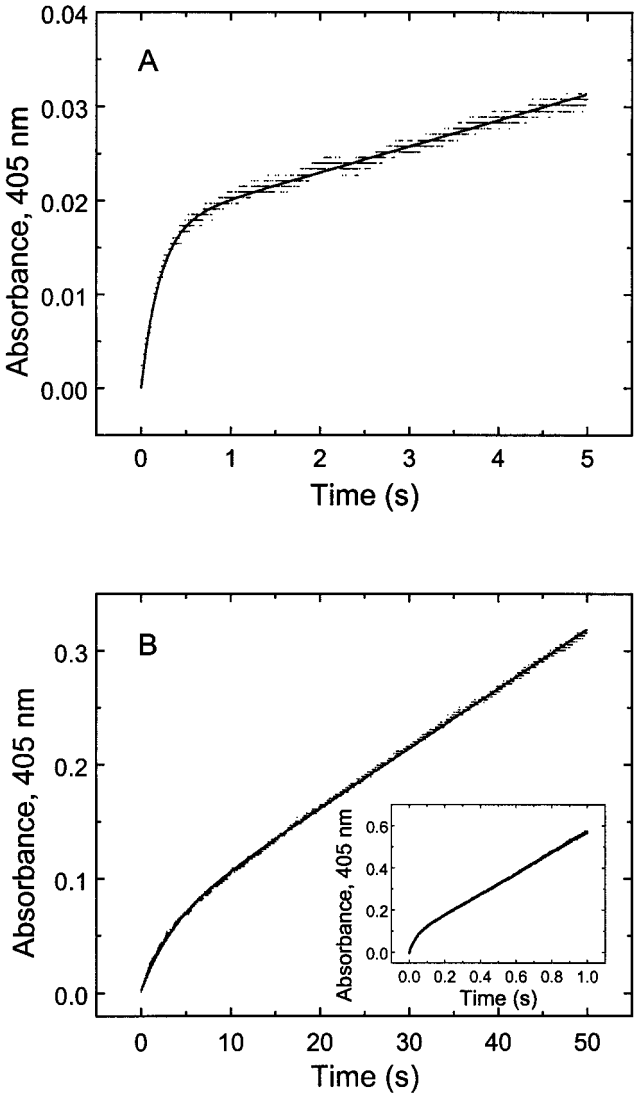

FIGURE 3: Burst kinetics observed with *Yersinia* PTPase (A) and VHR (B) at pH 6.0, 30 °C, using *p*NPP(S) as a substrate. The insert of (B) was burst kinetics observed with VHR using *p*NPP as a substrate. The final enzyme concentrations were 54 and 89 μM for *Yersinia* PTPase and VHR, respectively. The final substrate concentrations were 5 and 26 mM for *p*NPP(S) and *p*NPP, respectively. The specific rate constants are analyzed by fitting experimental data directly to the theoretical equation: $Absorbance_{405nm} = A \times T + B \times (1 - e^{-b \times t}) + C$ using the nonlinear least-squares fit algorithm in Origion 2.9.

the slow linear phase. Similar burst kinetics were observed for the PTP1B-catalyzed hydrolysis of *p*NPP(S), with rate constants for the burst phase and the slow phase of 2.8 and 0.051 s^{-1}, respectively. Because of the limited solubility and high background absorption at 405 nm, the highest *p*NPP(S) concentration after mixing was 5 mM. The burst stoichiometry and individual rate constants directly associated with the formation and breakdown of E−P(S) were determined as described in the Experimental Procedures. The results are listed in Table 4. As shown in Table 4, the burst stoichiometries observed in the stopped-flow experiments were similar to the calculated theoretical values, and the k_{cat} values determined from the pre-steady-state experiments agreed well with those determined from steady-state experiments (Table 1).

Because of the lower k_{cat} value, burst kinetics can be observed with VHR using *p*NPP as a substrate at pH 6 and

[3] Scheme 3 shows the proposed kinetic mechanism for the PTPase-catalyzed hydrolysis of *p*NPP(S). Concurrent with the expulsion of the leaving group, E−P(S) is formed, which is subsequently hydrolyzed to thiophosphate. Thiophosphate is then hydrolyzed through an E−P intermediate to generate inorganic phosphate and H_2S. Because thiophosphate hydrolysis and E−P hydrolysis are 5- and 5000-fold faster than the overall reaction, the burst kinetics data suggest that the rate-limiting step for the *p*NPP(S) reaction is E−P(S) hydrolysis.

Table 4: Pre-Steady-State Kinetic Parameters for the PTPase-Catalyzed Hydrolysis of *p*NPP and *p*NPP(S)[a]

		burst stoichiometry				
enzyme	substrate	calcd	obsd	k_2, (s^{-1})	k_3, (s^{-1})	k_{cat}, (s^{-1})
Yersinia PTPase	*p*NPP(S)	0.42	0.41	4.1 ± 0.5	0.073 ± 0.003	0.073 ± 0.003
PTP1B	*p*NPP(S)	0.42	0.32	3.7 ± 0.3	0.051 ± 0.003	0.051 ± 0.003
VHR	*p*NPP(S)	0.60	0.46	0.32 ± 0.02	0.064 ± 0.002	0.050 ± 0.001
VHR	*p*NPP	0.88	0.68	33 ± 2	5.3 ± 0.3	4.6 ± 0.02

[a] All experiments were conducted at pH 6.0 and 30 °C. *p*NPP(S) and *p*NPP concentrations were 5 and 26 mM, respectively. Burst stoichiometry = *B*/[E]. The theoretical amplitude of burst *B* was calculated from eq 2, and the observed amplitude of burst *B* was determined from the absorbance of the burst. k_2 and k_3 are rate constants for E−P or E−P(S) formation and hydrolysis, respectively, which were determined from eqs 3 and 4.

Scheme 3

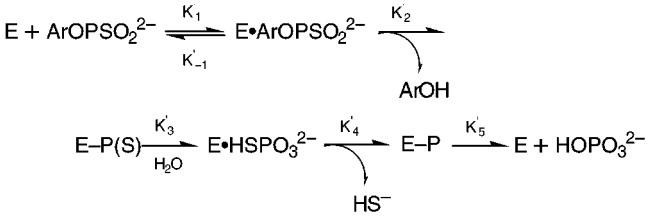

30 °C (*26*). To quantitatively compare the thio effect on both of the chemical steps, i.e. E−P or E−P(S) formation and breakdown, pre-steady-state kinetics were carried out for the VHR-catalyzed hydrolysis of both *p*NPP and *p*NPP(S) (Figure 3B). The rates for E−P formation (k_2) and breakdown (k_3) were 33 and 5.3 s^{-1}, respectively, in the VHR-catalyzed *p*NPP hydrolysis, which agreed well with previous measurements (*26*). In comparison, the rates for E−P(S) formation (k_2') and breakdown (k_3') were 0.32 and 0.064 s^{-1}, respectively, in the VHR-catalyzed *p*NPP(S) reaction. Although the k_{cat} for the VHR-catalyzed hydrolysis of *p*NPP(S) was 100-fold lower than *p*NPP, the rate of the intermediate formation was 5−6-fold faster than its hydrolysis for both substrates. This suggests that the replacement of a nonbridge oxygen with sulfur in *p*NPP slows down both chemical steps to a similar extent and does not change the rate-limiting step of the reaction.

pH Dependence of the PTPase-Catalyzed Hydrolysis of O−Arylphosphorothioates. The pH dependencies of k_{cat} and k_{cat}/K_m for the *Yersinia* PTPase-catalyzed hydrolysis of 3-nitrophenyl phosphate and 3-nitrophenyl phosphorothioate were compared. Because of the instability of the PTPase at pH < 5 and the low activity toward phosphorothioates, the expected variation in the low pH region of the k_{cat}/K_m − pH plot due to different substrate ionization constants were not observable. Nonetheless, the PTPase-catalyzed hydrolysis of 3-nitrophenyl phosphorothioate displayed similar pH-rate profiles to those of 3-nitrophenyl phosphate from pH 5−9, although the absolute value of k_{cat} and k_{cat}/K_m was about 5000-fold smaller at each pH (data not shown). Thus, substitution of a nonbridge oxygen with sulfur in *O*-aryl phosphate ester does not alter its pH-profile.

Leaving Group Dependence of the PTPase-Catalyzed Hydrolysis of O−Arylphosphorothioates. The leaving group dependence of the hydrolysis of *O*-arylphosphorothioates catalyzed by the *Yersinia* PTPase as well as VHR were investigated. For *O*-aryl phosphates the kinetic parameter k_{cat}/K_m monitors the E−P formation (*10*−*12*) and the kinetic parameter k_{cat} primarily follows the E−P hydrolysis (*26*, *30*, *36*; and this work). As shown in Figure 4, there was essentially no leaving group dependence in both k_{cat} and k_{cat}/K_m for the PTPase-catalyzed hydrolysis of *O*-arylphosphorothioates. The PTPase-catalyzed hydrolysis of *O*-aryl phosphates also exhibits no leaving group dependence on both k_{cat} and k_{cat}/K_m (*26*, *35*, *36*). The lack of leaving group dependence on k_{cat}/K_m can be attributed to essentially complete protonation of the phenolic oxygen in the leaving group by the general acid in the transition state for P−O bond cleavage (*10*−*12*, *27*). The lack of a leaving group effect on k_{cat} is consistent with the assignment of the hydrolysis of the covalent enzyme intermediate as rate-limiting (*36*).

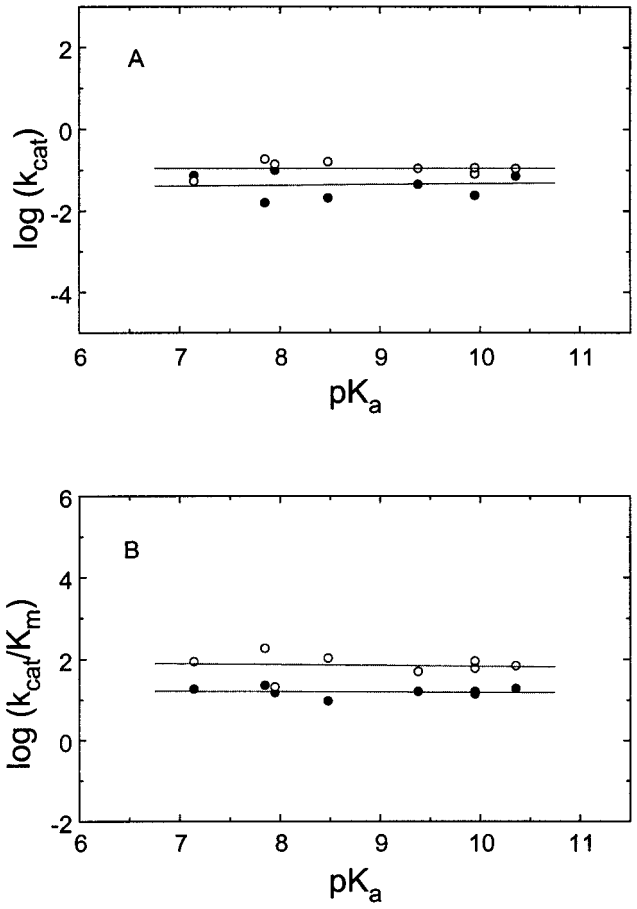

FIGURE 4: Leaving group dependence of the PTPases-catalyzed aryphosphorothioate monoester hydrolysis at pH 6.0, 30 °C. A: Leaving group dependence of k_{cat} for *Yersinia* PTPase (●), and VHR (○). B: Leaving group dependence of k_{cat}/K_m for *Yersinia* PTPase (●) and VHR (○). Values of the pK_a for the substituted phenols were from (39).

Solvent Isotope Effect. Proton transfer occurs in both of the chemical steps of the PTPase-catalyzed reaction (*1*). During the E−P formation step, the phenolate leaving group is protonated by the invariant Asp residue and during the

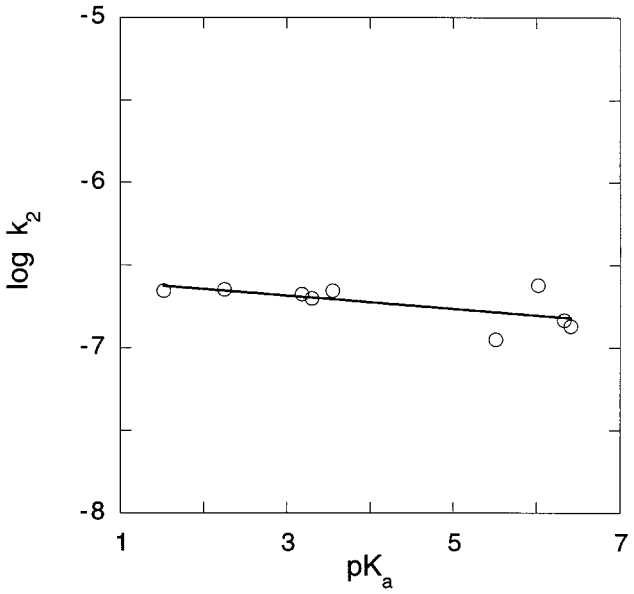

FIGURE 5: Logarithmic plot of second-order rate constants for hydrolysis of *p*NPP(S) dianion catalyzed by pyridine nucleophiles vs the pK_a of the pyridine nucleophile. The slope of the plot gives a β_{nuc} value of -0.04 ± 0.02. The pK_a values for the substituted pyridines are 1.52 (3-CN), 2.25 (4-CN), 3.30 (3-Cl), 3.18 (3-COCH3), 3.55 (3-CONH2), 5.51 (parent), 6.02 (3-CH3), 6.33 (4-CH3), and 6.41 (3,5-CH3) (*39*, *41*, *42*). (Conditions: $T = 37$ °C, pH 9.41, $I = 1$ M (KCl), 50 mM CHES, [S] = 55 μM).

E−P hydrolysis step, the nucleophilic water is deprotonated by the same Asp residue. Kinetic solvent isotope effects for the wild-type and Q446A mutant *Yersinia* PTPase-catalyzed hydrolysis of *p*NPP and *p*NPP(S) were measured. No significant D_2O solvent isotope effects were observed on k_{cat} and k_{cat}/K_m.

Comparison of the Transition State for the Nonenzymatic and the PTPase-Catalyzed Phosphoryl/Thiophosphoryl Transfer Reactions. To characterize the PTPase-catalyzed phosphorothioate reaction further, we determined the β_{nuc} values for both the solution and the enzymatic reactions. The Brønsted β_{nuc} value is the slope of the logarithm of the rate for a reaction vs the pK_a of the attacking nucleophiles and is often viewed as an approximate estimate of the extent of bond formation between the nucleophile and the reaction center in the transition state.

β_{nuc} Values for the Solution Reactions. The β_{nuc} value for the solution reaction of *p*NPP dianion with pyridine nucleophiles was found to be in the range of 0.13 to 0.18 (*33*, *40*). The dependence of the second-order rate constant on the basicity of nucleophile for the reaction between *p*NPP(S) and substituted pyridines is shown in Figure 5, which yields a β_{nuc} value of -0.04 ± 0.02. The smaller β_{nuc} value for the *p*NPP(S) reaction as compared to that for the *p*NPP reaction suggests that there is less nucleophilic involvement in the transition state for the *O*-phosphorothioate reaction. Stereochemical studies with chiral *p*NPP(S) show that the reaction proceeds with racemization, suggesting the existence of a monomeric thiometaphosphate intermediate in aqueous solution (*43*). A large volume of activation for the hydrolysis of 2,4-dinitrophenylphosphorothioate (*44*) and a large entropy of activation for *p*NPP(S) (*45*) have been observed, consistent with formation of a thiometaphosphate intermediate. In contrast, there is no direct evidence for the existence of a free metaphosphate intermediate in aqueous solutions (*46*).

Scheme 4

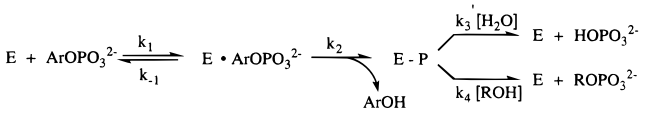

Collectively, the results suggest that the transition state for *O*-phosphorothioates is more dissociative than that for the oxygen analogues.

β_{nuc} Values for the PTPase Reactions. The transition state in the Stp1 phosphatase-catalyzed reaction has been characterized by studying the effect of changing alcohol basicity on its reactivity toward E−P (*13*). This is based on the property that the phosphoryl group in E−P can be transferred to water (hydrolysis) as well as alcohols. In the reaction catalyzed by the tyrosine-specific PTPases, the phosphoryl group cannot be transferred to nucleophiles other than water because of an invariant Gln residue (Gln446 in the *Yersinia* PTPase) in the active site that appears to position the hydrolytic water via a bidentate hydrogen bond (*25*, *47*). Replacement of Gln446 in the *Yersinia* PTPase by an Ala conferred phosphotransferase activity onto the phosphatase while exerting minimal effect on the hydrolytic activity (*25*). Observation of burst kinetics indicate that the rate-limiting step for k_{cat} in the Q446A-catalyzed hydrolysis of *p*NPP(S) is the breakdown of E−P(S) (data not shown), similar to that observed with the wild-type PTPase. These kinetic properties of the Q446A make it possible to probe the nature of the transition state of the *Yersinia* PTPase reactions.

In the presence of alcohols, the Q446A *Yersinia* PTPase-catalyzed *p*NPP(S) reaction produced alkyl thiophosphates in addition to the hydrolysis product (inorganic thiophosphate) (data not shown). Similarly, alkyl phosphates and inorganic phosphate were produced in the Q446A-catalyzed *p*NPP reaction in the presence of alcohols (*25*). Furthermore, alcohols stimulated the overall reactions for both *p*NPP and *p*NPP(S), consistent with the breakdown of E−P or E−P(S) being the rate-limiting step. This is not due to a general medium effect as in the concentration used (<1 M), alcohols have no effect in the wild-type *Yersinia* PTPase-catalyzed reaction. The presence of alcohols also did not have any effect on the rate of E−P hydrolysis by Q446A (*25*). Thus, the rate enhancements in alcohols are due to phosphoryl transfer to alcohols. To compare the transition states for the decomposition of E−P and E−P(S), the effect of nucleophile basicity on the second-order rate constant (k_4, Scheme 4) for the reaction of the β-substituted ethanols with E−P or E−P(S) was measured for the Q446A *Yersinia* PTPase. The selected β-substituted ethanols were all primary alcohols and had similar molecular volume such that the influence of steric and hydrophobic effects was minimized (*13*). A Brønsted plot of log k_4 against the pK_a of the attacking alcohol gave a β_{nuc} value of 0.06 ± 0.06 for the *p*NPP(S) reaction, slightly lower than the β_{nuc} value of 0.15 ± 0.05 for the *p*NPP reaction (Figure 6). β_{nuc} values alone cannot firmly establish the nature of a transition state. For example, the small observed values of β_{nuc} for reactions of E−P and E−P(S) not only are consistent with a dissociative transition state but also are consistent with general base-assisted proton removal coupled with bond formation. The following suggests that this latter possibility is unlikely. If there were significant proton transfer from the attacking alcohol or water

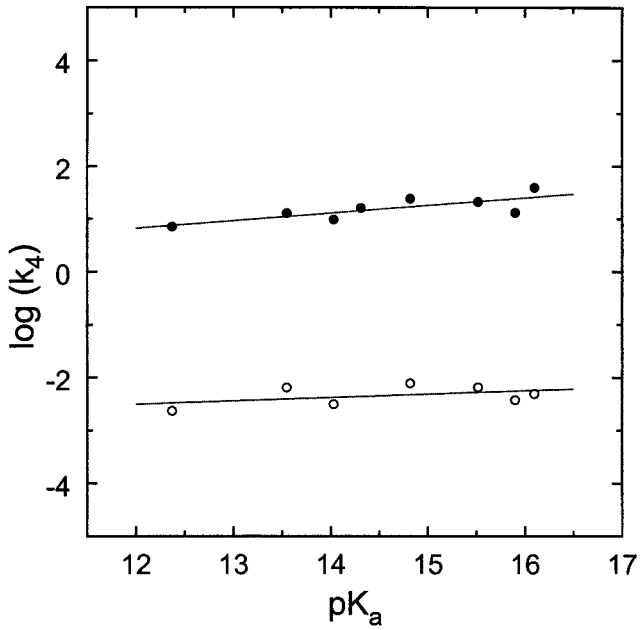

FIGURE 6: Brønsted plots of second-order rate constant (k_4, Scheme 4) for the alcoholysis of the enzyme-thiophosphate or enzyme-phosphate intermediate as a function of the basicity of the alcohols in the Q446A *Yersina* PTPase-catalyzed hydrolysis of *p*NPP(S) (○) and *p*NPP (●). Alcohols used were CF_3CH_2OH (pK_a 12.37), $HC{\equiv}CCH_2OH$ (pK_a 13.55), $N{\equiv}CCH_2CH_2OH$ (pK_a 14.03), $ClCH_2CH_2OH$ (pK_a 14.31), $CH_3OCH_2CH_2OH$ (pK_a 14.82), $CH_2{=}CHCH_2OH$ (pK_a 15.52), CH_3CH_2OH (pK_a 15.90), and $CH_3CH_2CH_2OH$ (pK_a 16.10). The pK_a values for the alcohols were from (*48*−*50*). All measurements were performed at 30 °C and pH 6.0, in 50 mM succinate, 1 mM EDTA, $I = 0.15$ M adjusted with NaCl.

to the general base during hydrolysis, then a larger β_{nuc} value would be predicted upon removal of the general base and a solvent isotope effect might be expected for E−P hydrolysis. However, alteration of the general base (D128E mutant of the Stp1 phosphatase) had no effect on the observed value of β_{nuc} (*13*). In addition, no significant solvent isotope effect was observed for k_{cat} for the wild-type and Q446A *Yersinia* PTPase reactions in which E−P hydrolysis is rate-limiting. Thus, the low β_{nuc} values are most simply interpreted in terms of little deprotonation from the nucleophile in a metaphosphate-like, dissociative transition state for hydrolysis of both E−P and E−P(S). Nevertheless, it should be noted that a distinct interpretation of linear free-energy realtionships for phosphoryl transfer reactions has recently been presented (*76*). The reader is referred to references (*8*, *9*, *54*, *77*) for further discussion of enzymatic transitions states for phosphoryl transfer. It appears that the nature of the transition state for the intermediate breakdown is dissociative for both reactions even though the rate of thiophosphotransfer from E−P(S) is 3 orders of magnitude slower than phosphotransfer from E−P (Figure 6). Thus, the transition states of the PTPases-catalyzed phosphoryl and thiophosphoryl transfer reactions appear to mirror those of the corresponding solution reactions,[4] supporting the notion that the transition state of the solution reaction is essentially the one stabilized by the enzyme leading to catalysis.

[4] Comparison between the β_{nuc} values of the enzyme reaction and the solution reaction is reasonable as the β_{nuc} values for O nucleophiles and the N nucleophiles in nonenzymatic phosphoryl transfer reactions are similar (*7*).

Thio Effects for PTPase Active-Site Mutants. The above results suggest that the two substrate classes react with PTPases via similar reaction pathways and transition states. The difference in reactivity presumably arises from differences in specific molecular interactions in the active site. This was tested by measuring the thio effect on k_{cat}/K_m for a number of site-directed mutant *Yersinia* PTPases. It has been shown that changes in the thio effect upon mutation of a particular side chain can be indicative of direct or indirect intermolecular interactions between the side chain and equatorial oxygens in the transition state (*51*−*54*). The use of single site mutant enzymes and modified substrates to gain insight into the interaction between the enzyme residue and the substrate is conceptually similar to the study of double enzyme mutants for potential interaction between the two residues (*55*). As shown in Table 5, the thio effects for the Q446A and Q450A reactions were similar to that of the wild-type. The thio effects for the D356A, W354A, and R409K mutants were reduced 8-, 22-, and 54-fold, respectively.

DISCUSSION

Thio Effect in Enzymatic and Nonenzymatic Reactions. Thio substitution accelerates the nonenzymatic hydrolysis of phosphate monoesters 10−60-fold (*14*−*16*) but decreases reaction rates of phosphate triesters 10−160-fold (*57*−*61*). This difference in thio effect is in accord with mechanistic differences, i.e. a primarily dissociative process in the monoester reactions but an associative one for the triester reactions (*9*). In contrast to the solution reaction, phosphorothioate monoesters are much poorer substrates than the oxygen analogues for a number of phosphoryl transfer enzymes, e.g. PTPases (this work), alkaline phosphatase (*14*, *62*), fructose bisphosphatase (*15*), protein kinases (*63*), and ATPases (*64*, *65*). The observed large thio effects were previously suggested, based on the large thio effect for the solution phosphotriester reactions, as evidence for an associative transition state for enzyme-catalyzed phosphoryl transfer reactions (*14*, *15*). However, differences in size, polarizability, electronegativity, hydrogen bonding, and affinity for metal ions between oxygen and sulfur (*66*−*68*) can cause differential interactions with the enzyme. The differences in interactions can obscure effects arising from intrinsic reactivity and thus prevent the use of thio effect as a readout for the enzymatic transition state (*17*).

Why PTPases Exhibit Large Thio Effects? To ensure that a thio effect for an enzyme reaction is interpreted properly, it is important that the reactions occur at the same active site, proceed with the same reaction pathway, and are rate-limited by chemistry. The PTPases provide an amenable system to gain an understanding of the chemical basis for the reduced reactivity of *O*-phosphorothioates in an enzyme reaction. The k_{cat}/K_m for the PTPase-catalyzed hydrolysis of aryl phosphates is limited by chemistry (*10*−*12*). With *p*NPP(S) as a substrate, the k_{cat} and k_{cat}/K_m values for the PTPases are 2−3 orders of magnitudes slower than those using *p*NPP as a substrate. This strongly suggests that chemistry is rate-limiting as well for the PTPase-catalyzed *O*-arylphosphorothioates reaction. This rendered it possible to characterize the transition state for both the PTPase-catalyzed phosphate and phosphorothioate reactions and

Table 5: Thio Effect on Catalysis by *Yersinia* PTPase and Its Active-Site Mutants

	*p*NPP		*p*NPP(S)			coupling
enzyme	k_{cat}/K_m, s^{-1} M^{-1}	ΔG^a, kcal/mol	k_{cat}/K_m, s^{-1} M^{-1}	ΔG^a, kcal/mol	thio effect[b]	$\Delta\Delta G^c$, kcal/mol
wild-type	$(1.3 \pm 0.1) \times 10^5$	0	26 ± 1	0	$5{,}000 \pm 400$	0
Q450A	$(1.2 \pm 0.1) \times 10^4$	1.4 ± 0.1	5.8 ± 0.2	0.90 ± 0.03	$2{,}100 \pm 100$	0.5 ± 0.1
Q446A	$(2.1 \pm 0.2) \times 10^5$	-0.29 ± 0.07	22 ± 1	0.10 ± 0.04	$9{,}500 \pm 1{,}000$	-0.39 ± 0.08
W354A	$(4.0 \pm 0.4) \times 10^2$	3.4 ± 0.1	1.7 ± 0.2	1.6 ± 0.1	230 ± 30	1.8 ± 0.1
D356A	$(3.0 \pm 0.1) \times 10^2$	3.6 ± 0.1	0.5 ± 0.1	2.4 ± 0.1	600 ± 120	1.2 ± 0.1
R409K	$(1.4 \pm 0.3) \times 10^1$	5.4 ± 0.1	0.15 ± 0.04	3.1 ± 0.2	93 ± 32	2.3 ± 0.2

[a] Apparent interaction free energy between the deleted side chain and the substrate in transition state, as calculated from the ratio of k_{cat}/K_m values of wild-type and the mutant under investigation, i.e. $\Delta G = -RT\ln[(k_{cat}/K_m)_{mutant}/(k_{cat}/K_m)_{WT}]$ (*56*). [b] The thio effect is defined as $(k_{cat}/K_m)_{pNPP}/(k_{cat}/K_m)_{pNPP(S)}$. [c] Energetic coupling between the mutation under investigation and the substrate's thio substitution. Values have been calculated from the difference in apparent interaction energy of a particular side chain with *p*NPP and *p*NPP(S), respectively: $\Delta\Delta G = \Delta G_{pNPP} - \Delta G_{pNPP(S)}$.

allowed a direct mechanistic comparison between the PTPase-catalyzed hydrolysis of aryl phosphates and *O*-arylphosphorothioates.

Inhibition studies and analysis with catalytically inactive PTPase indicate that the same active site is used for the hydrolysis of *O*-arylphosphorothioates and the corresponding phosphate esters. Results from pH and leaving group dependence measurements, D_2O solvent isotope effects, and burst kinetic experiments suggest that the same overall mechanism is employed for the PTPase-catalyzed hydrolysis of *O*-aryl phosphates and their sulfur-substituted analogues. Comparison of the affinity of *p*NPP and *p*NPP(S) for the PTPases suggest that thio substitution does not affect ground-state binding. Finally, Brønsted analyses coupled with previous observations (10−13) suggest that the transition states for the PTPase-catalyzed phosphoryl and thiophosphoryl transfer are highly dissociative, similar to the corresponding solution reactions (see Results). Thus, the rate decrease for the enzyme-catalyzed phosphoryl transfer reaction upon thio substitution does not provide evidence for an associative, triester-like transition state. The results provide strong evidence that the large thio effect observed in the PTPase reaction is caused by less favorable interactions of the active site with the phosphorothioate group in the transition state as compared to the normal phosphate reaction.

Thio Effects Highlight the Importance of Transition State Complementarity. X-ray structural studies have shown that the phosphoryl group in the substrate is coordinated by multiple hydrogen bonds with the main-chain amide groups of the PTPase-signature motif. In addition, the side chain of the invariant Arg residue (Arg409 in the *Yersinia* PTPase), which is located in the same PTPase-signature motif, forms a bidentate hydrogen bond with two of the nonbridge phosphoryl oxygens (*69*, *70*). When Arg409 was replaced with an Ala, an 8200-fold decrease in k_{cat} and a 26-fold increase in K_m were observed for *p*NPP. The R409K mutant displayed a k_{cat} value identical to that of R409A, but the apparent K_m value for *p*NPP was only 1.9-fold higher than that of the wild-type enzyme (*4*). The ability of Lys to effectively substitute for Arg in substrate binding but not in catalysis suggests that PTPases likely employ the unique structural properties of the guanidinium side chain of the arginine to preferentially stabilize the transition state. The ability of the guanidinium group to form a coplanar bidentate complex with two of the equatorial oxygen atoms present on the phosphate during catalysis provides a plausible mechanism for stabilization of the trigonal bipyramidal transition state (*4*).

The model depicted in Figure 7 can explain the differential effects of thio substitution on ground-state and transition-state binding. As thio substitution does not affect substrate binding, it appears that a larger sulfur atom at the terminal position can be tolerated in the ground-state complex. However, enzymes effect catalysis by stabilizing the transition state, which is accomplished by precise geometric and electrostatic alignment between the reacting groups in the substrate and the enzyme (*71*). With a sulfur substitution in phosphorothioates, because of its larger size, the precise alignment between the substrate and the enzyme in the transition state is presumably disrupted, giving rise to the observed large thio effect.

To test this hypothesis directly and to provide functional evidence for the interaction between the active-site Arg and the phosphoryl moiety at the transition state, the thio effect was measured for the R409K mutant. Site-directed mutagenesis of the contact points with the substrate thiophosphoryl group and PTPase probes disruption of molecular recognition in the transition state by thio-substitution. Replacement of Arg409 by a Lys decreased the thio effect by 54-fold, corresponding to an energetic coupling between the R409K mutation and the thio substitution of 2.3 kcal/mol (Table 5). This is consistent with a direct interaction between the side chain of Arg409 and the equatorial oxygens in the transition state. According to the model (Figure 7), the reduction in thio effect for R409K results because Arg409 cannot interact well with the bulkier sulfur-containing thiophosphoryl group in the transition state, so that the catalytic contribution of this residue is markedly reduced for the thio substrate.

Asp356 is the general acid/base (*5*, *27*) that interacts with the apical oxygen of vanadate, which most closely resembles the leaving group oxygen or the attacking water in the transition state (*47*, *72*, *73*). Trp354 is important for the positioning of Arg409 and Asp356 in a catalytically competent conformation (*28*, *74*). Although Asp356 and W354 do not make direct contact with the sulfur atom, they are likely important for the proper alignment of the substrate or active-site residues in the transition state. If the precise transition state alignment is disrupted by the thio substituted substrate in the active site, mutation of residues important for the active-site integrity should result in smaller effect on catalysis (*54*). D356A and W354A mutants displayed thio effects 8- and 22-fold smaller than the wild-type enzyme, corresponding to energetic coupling of 1.2 and 1.8 kcal/mol,

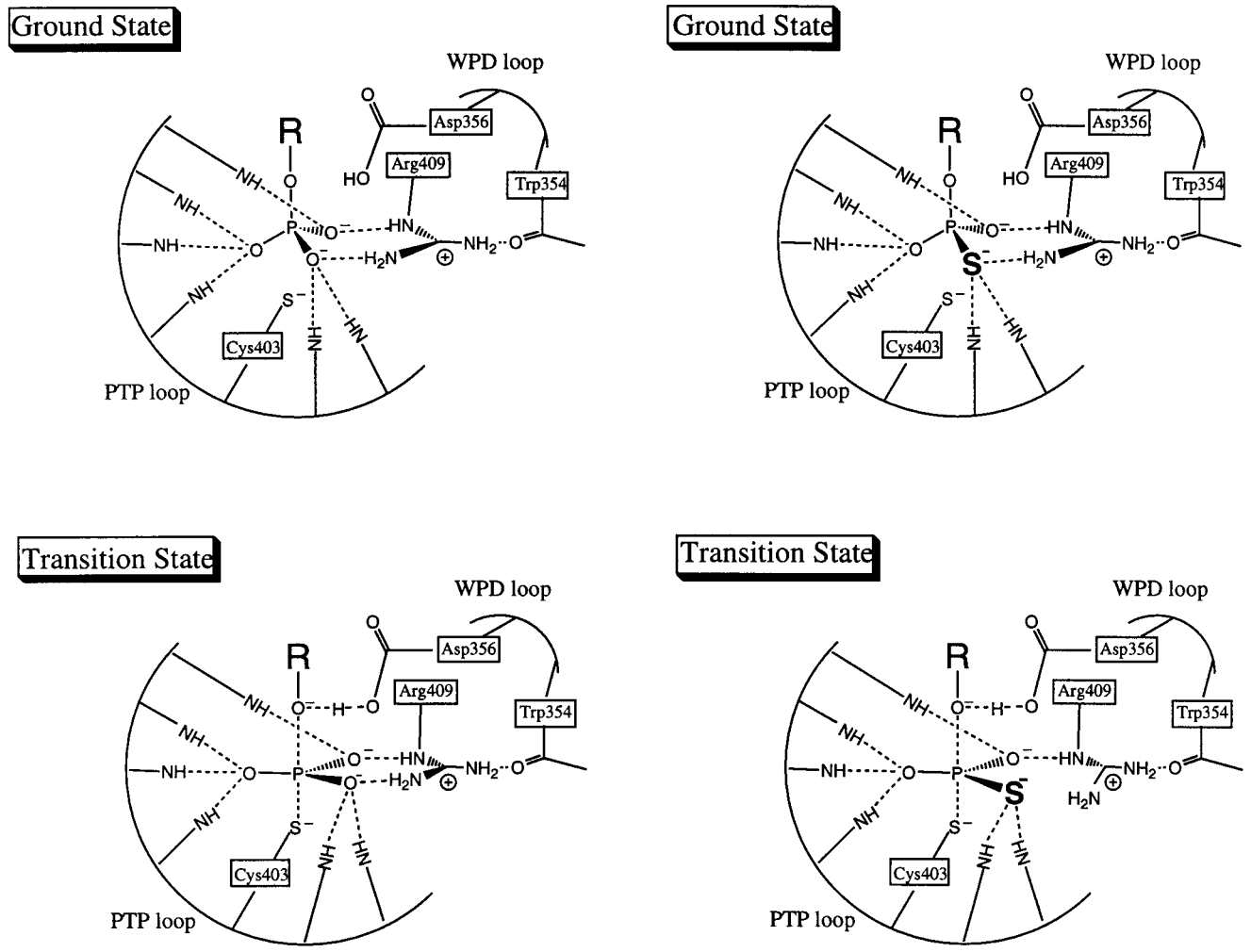

FIGURE 7: A model for the differential thio effects for ground-state and transition-state binding of phosphorothioates. The drawings are based on the crystal structure of the *Yersinia* PTPase (*69*). For O-aryl phosphates, the nonbridge phosphoryl oxygens form shorter and stronger hydrogen bonds with the amides of the active-site loop and the side chain of Arg409 in the transition state. In addition, the bidentate hydrogen bond between Arg409 and two of the phosphoryl oxygens is coplanar in the transition state (*73*, *75*). For O-arylphosphorothioates, it is difficult to achieve the same complementarity or alignment in the active site with the larger sulfur atom. Because of the preferential stabilization of the trigonal bipyramidal transition state by the PTPase's active site, the disruption of the alignment and hydrogen bonding network by sulfur substitution is more severe in transition state than ground state. Thus, the large thio effect observed for the wild-type *Yersinia* PTPase is presumably due to the bulkier sulfur substituent in O-arylphosphorothioates, which disrupts the hydrogen bonds between the active-site and the substrate in the transition state.

respectively (Table 5). These changes in thio effects reflecting indirect interactions highlight the importance of the overall correct transition state alignment. As a control, we also determined the thio effects for Q446A and Q450A. There are no direct interactions between the two Gln residues and the equatorial oxygens. Q446A and Q450A had kinetic constants similar to those of the wild-type enzyme (*25*) and thio effects similar to that of the wild-type. Collectively, the reduced thio effect for the R409K mutant, combined with previous structural data, provides direct evidence for the role of Arg409 in transition state stabilization. We conclude that the alignment and hydrogen bonding network between the substrate and the PTPase in the transition state are disrupted when a phosphoryl oxygen is replaced by a bigger sulfur, resulting in the large thio effect.

Why Is Complementarity So Important? Structural studies showed that the hydrogen-bonding distance between the amides and the active-site Arg residue of the PTPase-signature motif and equatorial oxygens in vanadate, which has a trigonal bipyramid geometry analogous to the transition state, were reduced on average by 0.12−0.18 Å when compared with tetrahedral phosphate ion bound in the bovine low molecular weight tyrosine phosphatase (*73*). In addition, molecular dynamics simulations suggested that PTPases stabilized the transition state through Walden-inversion-enforced hydrogen-bonding interactions in the active-site (*75*). The hydrogen bonding distances between the phosphoryl oxygens and the side chain of the invariant Arg and the main chain amides of the PTPase-active-site loop were found to be shortened by 0.05−0.1 Å from the ground state

to the transition state. This is due to spatial expansion of the three nonbridging oxygen atoms in going from the tetrahedral reactant state to a trigonal bypyramidal geometry at the transition state.

The ability of the guanidinium group of the active-site Arg residue and the phosphate binding loop to form shorter and stronger hydrogen bonds with the equatorial oxygen atoms in the transition state than the terminal oxygens in the ground state provides a potential structural basis for the preferential stabilization of the trigonal bipyramidal transition state(s). This ability is compromised by the bulky sulfur substitution in *p*NPP(S) or E−P(S), which disrupts hydrogen bonding interactions between the equatorial atoms and the phosphate binding loop (including Arg409) in the transition state (Figure 7). The large thio effect for *O*-phosphorothioates in PTPase reaction thus appear to result from an impaired ability to attain the optimal geometry for transition state stabilization.

Conclusion. This work provides a thorough characterization of the PTPase-catalyzed *O*-phosphorothioates. The PTPases-catalyzed hydrolysis of *O*-arylphosphorothioates is 2−3 orders of magnitude slower than that of *O*-aryl phosphates. The same mechanism and dissociative transition state are utilized for both classes of substrates. Thio effects for the wild-type and mutant *Yersinia* PTPases combined with previous results suggest an important role for Arg409 in transition-state stabilization. Substitution of a nonbridge phosphoryl oxygen by a bulkier sulfur apparently disrupts the precise geometric alignment and hydrogen bonding network between the substrate and the enzyme active site in the transition state, resulting in low activity of PTPases toward *O*-arylphosphorothioates.

ACKNOWLEDGMENT

We thank Drs. Alvan Hengge and Chris Walsh for reading and comments on the manuscript.

REFERENCES

1. Zhang, Z.-Y. (1998) *CRC Crit. Rev. Biochem. Mol. Biol. 33*, 1−52.
2. Guan, K. L., and Dixon, J. E. (1991) *J. Biol. Chem. 266*, 17026−17030.
3. Cho, H., Krishnaraj, R., Kitas, E., Bannwarth, W., Walsh, C. T., and Anderson, K. S. (1992) *J. Am. Chem. Soc. 114*, 7296−7298.
4. Zhang, Z.-Y., Wang, Y., Wu, L., Fauman, E., Stuckey, J. A., Schubert, H. L., Saper, M. A., and Dixon, J. E. (1994) *Biochemistry 33*, 15266−15270.
5. Zhang, Z.-Y., Wang, Y., and Dixon, J. E. (1994) *Proc. Natl. Acad. Sci. U.S.A. 91*, 1624−1627.
6. Benkovic, S. J., and Schray, K. J. (1978) in *Transition States of Biochemical Processes*, (Gandour, R. D., and Schowen, R. L., Ed.) pp 493−527, Plenum Press, New York.
7. Herschlag, D., and Jencks, W. P. (1989) *J. Am. Chem. Soc. 111*, 7579−7586.
8. Thatcher, G. R. J., and Kluger, R. (1989) *Adv. Phys. Org. Chem. 25*, 99−265.
9. Cleland, W. W., and Hengge, A. C. (1995) *FASEB J. 9*, 1585−1594.
10. Hengge, A. C., Sowa, G, Wu, L., and Zhang, Z.-Y. (1995) *Biochemistry 34*, 13982−13987.
11. Hengge, A. C., Denu, J. M., and Dixon, J. E. (1996) *Biochemistry 35*, 7084−7092.
12. Hengge, A. C., Zhao, Y., Wu, L., and Zhang, Z.-Y. (1997) *Biochemistry 36*, 7928−7936.
13. Zhao, Y., and Zhang, Z.-Y. (1996) *Biochemistry 35*, 11797−11804.
14. Breslow, R., and Katz, I. (1968) *J. Am. Chem. Soc. 90*, 7376−7377.
15. Domanico, P., Mizrahi, V., and Benkovic, S. J. (1986) in *Mechanisms of Enzymatic Reactions*: *Stereochemistry* (Frey, P. A., Ed.) pp 127−138, Elsevier, New York.
16. Hollfelder, F., and Herschlag, D. (1995) *Biochemistry 34*, 12255−12264.
17. Herschlag, D., Piccirilli, J. A., and Cech, T. R. (1991) *Biochemistry 30*, 4844−4854.
18. Cassel, D., and Glaser, L. (1982) *Proc. Natl. Acad. Sci. U.S.A.* 79, 2231−2235.
19. Tonks, N. K., Diltz, C. D., and Fischer, E. H. (1988) *J. Biol. Chem. 263*, 6722−6730.
20. Cho, H., Krishnaraj, R., Itoh, M., Kitas, E. Bannwarth, W., Saito, H., and Walsh, C. T. (1993) *Protein Sci. 2*, 977−984.
21. Zhang, Z.-Y., Maclean, D., McNamara, D. J., Sawyer, T. K., and Dixon, J. E. (1994) *Biochemistry 33*, 2285−2290.
22. Hiriyanna, K. T., Baedke, D., Baek, K.-H., Forney, B. A., Kordiyak, G., and Ingebritsen, T. S. (1994) *Anal. Biochem. 223*, 51−58.
23. Zhao, Z. (1996) *Biochem. Biophys. Res. Commun. 218*, 480−484.
24. Zhang, Y.-L., Keng, Y.-F., Zhao., Y., Wu., L., and Zhang, Z.-Y. (1998) *J. Biol. Chem. 273*, 12281−12287.
25. Zhao, Y., Wu, L., Noh, S. J., Guan, K.-L., and Zhang, Z.-Y. (1998) *J. Biol. Chem. 273*, 5484−5492.
26. Zhang, Z.-Y., Wu, L., and Chen, L. (1995) *Biochemistry 34*, 16088−16096.
27. Wu, L., and Zhang, Z.-Y. (1996) *Biochemistry 35*, 5426−5434.
28. Keng, Y.-F., and Zhang, Z.-Y. (1999) *Eur. J. Biochem. 259*, 809−814.
29. Zhang, Z.-Y., and Van Etten, R. L. (1991) *J. Biol. Chem. 266*, 1516−1525.
30. Zhang, Z.-Y., Palfey, B. A., Wu., L., and Zhao, Y. (1995b) *Biochemistry 34*, 16389−16396.
31. Bender, M. L., Kezdy, F. J., and Wedler, F. C. (1967) *J. Chem. Edu. 44*, 84−88.
32. Quinn, D. M., and Suffor, L. D. (1991) in *Enzyme Mechanism from Isotope Effects* (Cook, P. F., Ed.) pp 73−126, CRC Press, Boca Raton, FL.
33. Kirby, A. J., and Jencks, W. P. (1965) *J. Am. Chem. Soc. 87*, 3209−3216.
34. Zhang, Z.-Y., and Wu, L. (1997) *Biochemistry 36*, 1362−1369.
35. Zhang, Z.-Y., Malochowski, W. P., Van Etten, R. L., and Dixon, J. E. (1994) *J. Biol. Chem. 269*, 8140−8145.
36. Zhang, Z.-Y. (1995) *J. Biol. Chem. 270*, 11199−11204.
37. Dittmer, D. C., and Ramsay, O. B. (1963) *J. Org. Chem. 28*, 1268−1272.
38. Chlebowski, J. F., and Coleman, J. E. (1974) *J. Biol. Chem. 249*, 7192−7202.
39. Jencks, W. P., and Regenstein, J. (1970) in *CRC Handbook of Biochemistry*, pp J-187 − J-244, Cleveland, OH.
40. Herschlag, D., and Jencks, W. P. (1987) *J. Am. Chem. Soc. 109*, 4665−4674.
41. Skoog, M. T., and Jencks, W. P. (1984) *J. Am. Chem. Soc. 106*, 7597−7606.
42. Labow, B. I., Herschlag, D., and Jencks, W. P. (1993) *Biochemistry 32*, 8737−8741.
43. Cullis, P. M., Mirsa, R., and Wilkins, D. J. (1987) *J. Chem. Soc. Chem. Commun*. 1594−1596.
44. Burgess, J., Blundell, N., Cullis, P. M., Hubbard, C. D., and Misra, R. (1988) *J. Am. Chem. Soc. 110*, 7900−7901.
45. Catrina, I. E., and Hengge, A. C. (1999) *J. Am. Chem. Soc. 121*, 2156−2163.
46. Herschlag, D., and Jencks, W. P. (1986) *J. Am. Chem. Soc. 108*, 7938−7946.
47. Pannifer, A. D. B., Flint, A. J., Tonks, N. K., and Barford, D. (1998) *J. Biol. Chem. 273*, 10454−10462.
48. Ballinger, P., and Long, F. A. (1960) *J. Am. Chem. Soc. 82*, 795−798.
49. Murto, J. (1964) *Acta. Chem. Scand. 18*, 1043−1053.

50. Takahashi, S., Cohen, L. A., Miller, H. K., and Peake, E. G. (1971) *J. Org. Chem. 36*, 1205−1209.
51. Hondal, R. J., Bruzik, K. S., Zhao, Z., and Tsai, M.-D. (1997) *J. Am. Chem. Soc. 119*, 5477−5478.
52. Hondal, R. J., Zhao, Z., Riddle, S. R., Kravchuk, A. V., Liao, H., Bruzik, K. S., and Tsai, M.-D. (1997) *J. Am. Chem. Soc. 119*, 9933−9934.
53. Loverix, S., Winquist, A., Strömberg, R., and Steyaert, J. (1998) *Nature Struct. Biol. 5*, 365−368.
54. Admiraal, S. J., Schneider, B., Meyer, P., Janin, J., Veron, M., Deville-Bonne, D., and Herschlag, D. (1999) *Biochemistry 38*, 4701−4711.
55. Mildvan, A. S., Weber, D. J., and Kuliopulos, A. (1992) *Arch. Biochem. Biophys. 294*, 327−340.
56. Fersht, A. R. (1988) *Biochemistry 27*, 1577−1580.
57. Ketelaar, J. A. A., Gersmann, H. R., and Koopsmans, K. (1952) *Recl. Trav. Chim. 71*, 1253−1258.
58. Heath, D. F. (1956) *J. Chem. Soc.*, 3796−3804.
59. Heath, D. F. (1956) *J. Chem. Soc.*, 3804−3809.
60. Cox, J. R., Jr., and Ramsay, O. B. (1964) *Chem. Rev. 64*, 317−351.
61. Fanni, T., Taira, K., Gorenstein, D. G., Vaidyanathaswany, R., and Verkade, J. G. (1986) *J. Am. Chem. Soc. 108*, 6311−6314.
62. Neuman, H. (1968) *J. Biol. Chem. 243*, 4671−4676.
63. Grace, M. R., Walsh, C. T., and Cole, P. A. (1997) *Biochemistry 36*, 1874−1881.
64. Webb, M. R., Grubmeyer, C., Penefsky, H. S., and Trentham, D. R. (1980) *J. Biol. Chem. 255*, 11637−11639.
65. Webb, M. R., and Trentham, D. R. (1980) *J. Biol. Chem. 256*, 4884−4887.
66. Cohn, M. (1982) *Acc. Chem. Res. 15*, 326−332.
67. Frey, P. A., and Sammons, R. D. (1985) *Science 228*, 541−545.
68. Eckstein, F. (1985) *Annu. Rev. Biochem. 54*, 367−402.
69. Stuckey, J. A., Schubert, H. L, Fauman, E. B., Zhang, Z.-Y., Dixon, J. E., and Saper, M. A. (1994) *Nature 370*, 571−575.
70. Jia, Z., Barford, D., Flint, A. J., and Tonks, N. K. (1995) *Science 268*, 1754−1758.
71. Jencks, W. P. (1975) *Adv. Enzymol. 43*, 219−410.
72. Denu, J. M., Lohse, D. L., Vijayalakshmi, J., Saper, M. A., and Dixon, J. E. (1996) *Proc. Natl. Acad. Sci. USA 93*, 2493−2498.
73. Zhang, M., Zhou, M., Van Etten, R. L., and Stauffacher, C. V. (1997) *Biochemistry 36*, 15−23.
74. Schubert, H. L., Fauman, E. B., Stuckey, J. A., Dixon, J. E., and Saper, M. A. (1995) *Protein Sci. 4*, 1904−1913.
75. Alhambra, C., Wu, L., Zhang, Z.-Y., and Gao, J. (1998) *J. Am. Chem. Soc. 120*, 3858−3866.
76. Åqvist, J., Kolmodin, K., Florian, J., and Warshel, A. (1999) *Chem. Biol. 6*, R71−R80.
77. Mildvan, A. S. (1997) *PROTEINS*: *Structure, Function, and Genetics 29*, 401−416.

BI990836I